

Research



Cite this article: Hao Y, Wang Q, Li J, Yang S, Zheng Y, Peng W. 2022 Double nicking by RNA-directed Cascade-nCas3 for high-efficiency large-scale genome engineering. *Open Biol.* **12**: 210241.

<https://doi.org/10.1098/rsob.210241>

Received: 16 August 2021

Accepted: 15 November 2021

Subject Area:

biotechnology/molecular biology/genetics

Keywords:

Cas3 nickase, genome editing, high-efficiency, CRISPR-Cas, large genomic fragments deletion

Authors for correspondence:

Yanli Zheng

e-mail: yanli.zheng@whpu.edu.cn

Wenfang Peng

e-mail: wenfang@hubu.edu.cn

Electronic supplementary material is available online at <https://doi.org/10.6084/m9.figshare.c.5752434>.

Double nicking by RNA-directed Cascade-nCas3 for high-efficiency large-scale genome engineering

Yile Hao^{1,2}, Qinhuang Wang², Jie Li², Shihui Yang², Yanli Zheng¹ and Wenfang Peng²

¹College of Life Science and Technology, Wuhan Polytechnic University, Wuhan 430023, People's Republic of China

²State Key Laboratory of Biocatalysis and Enzyme Engineering, Hubei Engineering Research Center for Bio-enzyme Catalysis, Environmental Microbial Technology Center of Hubei Province, Hubei Collaborative Innovation Center for Green Transformation of Bio-resources, School of Life Sciences, Hubei University, Wuhan 430062, People's Republic of China

YZ, 0000-0001-5923-773X; WP, 0000-0001-9073-1509

New CRISPR-based genome editing technologies are developed to continually drive advances in life sciences, which, however, are predominantly derived from systems of Type II CRISPR-Cas9 and Type V CRISPR-Cas12a for eukaryotes. Here we report a novel CRISPR-n(nickase)Cas3 genome editing tool established upon a Type I-F system. We demonstrate that nCas3 variants can be created by alanine-substituting any catalytic residue of the Cas3 helicase domain. While nCas3 overproduction via plasmid shows severe cytotoxicity, an *in situ* nCas3 introduces targeted double-strand breaks, facilitating genome editing without visible cell killing. By harnessing this CRISPR-nCas3 *in situ* gene insertion, nucleotide substitution and deletion of genes or genomic DNA stretches can be consistently accomplished with near-100% efficiencies, including simultaneous removal of two large genomic fragments. Our work describes the first establishment of a CRISPR-nCas3-based genome editing technology, thereby offering a simple, yet useful approach to convert the naturally most abundantly occurring Type I systems into advanced genome editing tools to facilitate high-throughput prokaryotic engineering.

1. Introduction

CRISPR-Cas systems are a group of RNA-guided machineries that defend their prokaryotic hosts against invasive genetic elements in a programmable manner [1,2]. The targetable DNA-binding Cas nucleases are therein applied in generating double-stranded DNA breaks (DSBs) at specific chromosomal loci, stimulating the host repair mechanisms, including homology-directed repair (HDR) and non-homologous end joining (NHEJ), to bring about designed or error-prone genomic alterations [3]. Such applications have been currently focused on the compact Class 2 systems with a single Cas effector on account of their simplicity and hence ease of heterologous use [4]. Among Class 2 systems, the notable CRISPR-Cas9 from *Streptococcus pyogenes* has pioneered successful genome editing in various organisms or cell lines [5,6]. The success of wild-type Cas9-based applications has also fuelled the development of the technologies based on its derivatives, such as the nCas9 (Cas9 nickase) that possesses several advantages over the original [3]. For instance, a paired-nCas9 strategy can be used to greatly enhance DNA targeting specificity and consequently lower off-targeting in genome editing [7]. Additionally, nCas9 can help deaminases to yield more predictable and precise genome editing compared with wild-type Cas9-based editing [8].

Despite the versatility and robustness of the CRISPR-Cas9/nCas9 technologies, their applications in prokaryotes have been rather limited, because overexpressing

the exogenous Cas proteins in most bacteria could be cytotoxic and would lead to failure in yielding colonies [9]. As an alternative strategy, several Type I CRISPR-Cas3 systems belonging to Class 1 have been exploited to work as 'built-in' genome editing tools in their native hosts [10,11], including Type I-A of *Sulfolobus islandicus* [12], Type I-B of *Haloarcula hispanica* [13] and *Clostridium* species [14,15], Type I-C of *Pectobacterium aeruginosa* [16], Type I-E of *Streptococcus thermophilus* [17] and *Lactobacillus crispatus* [18], and Type I-F of *Pectobacterium* species [19,20] and *Zymomonas mobilis* [21], where the processive Cas3 nuclease-helicase was used to generate chromosomal breaks. Recent studies have also employed Type I-D and I-E systems for DNA cleavage in plants [22] and human cells [23–25], respectively, and Type I-E and I-F systems for gene expression modulation in human cells [26,27], further broadening the applicability of CRISPR-Cas3-based technologies. These accomplishments have paved a new possibility to develop advanced CRISPR-nCas3 toolkits based on endogenous Type I systems. Yet, to the best of our knowledge, no CRISPR-nCas3-based technology has been currently available.

We have previously accomplished genome engineering with the endogenous Type I-F CRISPR-Cas3 system of *Z. mobilis* ZM4. In the work, the editing options concerning single genes, including knockout, replacement and *in situ* nucleotide substitutions, yielded 100% efficiencies, whereas others did not; for example, at most 50% efficiency could be achieved in the deletion of a large genomic fragment (approx. 10 kb; ca 0.5% of the genome) [21]. Here we have, for the first time, developed a CRISPR-nCas3 genome editing tool, which has enabled large-scale genomic deletions with near-100% efficiencies that is currently hardly achievable using other methodologies. In addition, this tool has allowed for simultaneous deletion of two large genomic fragments with an efficiency of up to 75%, showing its great potential to serve as a versatile tool for high-throughput genome engineering.

2. Material and methods

2.1. Strains, growth conditions and electroporation of *Zymomonas mobilis*

Zymomonas mobilis ZM4 and derivatives constructed in this work were listed in electronic supplementary material, table S1. *Z. mobilis* strains were grown at 30°C in an RMG medium (20 g l⁻¹ glucose, 10 g l⁻¹ yeast extract, 2 g l⁻¹ KH₂PO₄). If required, spectinomycin was supplemented to a final concentration of 200 µg ml⁻¹ for *Z. mobilis* and 50 µg ml⁻¹ for *Escherichia coli*. Competent cells of *Z. mobilis* were prepared as previously described [28] and transformed with plasmids by electroporation using Bio-Rad Gene Pulser (0.1 cm gap cuvettes, 1.6 kV, 200 Ω, 25 µF) (Bio-Rad, Hercules, CA, USA) following the method developed for *Z. mobilis* [29]. Electroporated cells were incubated in an RMG2 medium for 3 h at 30°C prior to plating.

2.2. Construction of plasmids

Artificial CRISPR expression plasmids were constructed based on the *E. coli*-*Z. mobilis* shuttle vector, pEZ15Asp [28]. A DNA block consisting of the leader sequence of the chromosomal CRISPR2 as a promoter and three CRISPR repeats separated by two BsaI and two BsmBI restriction sequences in opposite

orientation, respectively, was synthesized from GenScript (Nanjing, China) and used as a template for PCR amplification with the primer pair of L3R-XbaI-F/L3R-EcoRI-R. Then, the PCR product was digested with XmaI and BamHI, and subsequently inserted into the pEZ15Asp vector, generating the base vector pL3R. Digestion of pL3R with BsaI generated a linearized plasmid having protruding repeat sequences of 4 nt at both ends. Double-stranded spacer DNAs were prepared by annealing two spacer oligonucleotides through being heated to 95°C for 5 min followed by cooling down gradually to room temperature. Likewise, the second spacer could be inserted in between the repeats by using the BsmBI sites. The spacer fragments were designed to correspondingly carry protruding ends complementary to those in the linearized vector. Therefore, self-targeting plasmids each bearing an artificial CRISPR with two self-targeting spacers were generated by gradually ligating spacer inserts with the linearized vectors. By repeating the reactions, the pRMV plasmid for simultaneously removing the two large genomic fragments was yielded. Subsequently, donor DNA fragments each containing a mutant allele of a target gene were generated by splicing and overlap extension PCR (SOE-PCR) [30] and individually cloned into their cognate self-targeting plasmids through the T5 exonuclease-dependent DNA assembly method [31]. Genome editing plasmids for creating the nCas3 mutants were constructed based on the pL2R plasmid vector following the previously described method [21].

Expression plasmids of Cas3 and Cascade proteins were constructed with the *E. coli* pET28a expression vector. Individual *cas* gene was PCR-amplified from *Z. mobilis* total DNA using specific primers listed in electronic supplementary material, table S1. The PCR product of *cas3* gene was used as a template to amplify the mutant genes through SOE-PCR [30] using primers listed in electronic supplementary material, table S2 containing the corresponding mutations. After being digested with the enzymes indicated in each PCR primer, the DNA fragments were individually cloned to pET28a at compatible sites, giving pET-Cas3, pET-Cas5, pET-Cas6, pET-Cas7, pET-Cas8, pET-K458A, pET-D608A and pET-R887A.

For overexpression of the Cas3 variants in *Z. mobilis*, each gene was amplified from the pET-K458A, pET-D608A and pET-R887A, respectively, using specific primers listed in electronic supplementary material, table S2, and clone to the pEZ15Asp vector or the genome editing plasmid pKO-ZMO0038n at EcoRI and XbaI sites, yielding pEZ-K458A, pEZ-D608A and pEZ-R887A, or pKO-ZMO0038-K458A, pKO-ZMO0038-D608A and pKO-ZMO0038-R887A, respectively.

All plasmids were listed in electronic supplementary material, table S1. All oligonucleotides were synthesized from GenScript (Nanjing, China) and listed in electronic supplementary material, table S2. Restriction enzymes and T5 exonuclease were purchased from New England Biolabs (Beijing) Ltd (Beijing, China).

2.3. Expression and purification of Cas proteins

The Cas expression plasmids were individually transformed into *E. coli* BL21 (DE3) and expression of the His-tagged Cas proteins was performed following the instruction of the protein purification kit (Qiagen, Valencia, CA, USA). Single colonies of transformed cells were cultivated overnight, followed by 1/100 dilution into 100 ml of LB media containing 100 µg ml⁻¹ ampicillin. The cells were firstly incubated at

37°C to an OD₆₀₀ of 0.6–0.8, then transferred to a shaker and induced with isopropyl β-D-1-thiogalactopyranoside in a final concentration of 0.5 mM at 16°C. After continuously shaking for 22 h, cells were harvested, lysed and purified using Ni-NTA resin (Qiagen, Valencia, CA, USA). The purified proteins were desalted with desalting column (GE Healthcare, Chicago, IL, USA) using AKTA system (GE Healthcare, Chicago, IL, USA), and finally confirmed by SDS-PAGE electrophoresis. Throughout purification, we used a buffer containing 20 mM HEPES (pH 7.5), 75 mM NaCl, 1 mM DTT and 2 mM EDTA for lysis, washing and elution.

2.4. Plasmid DNA cleavage assay

A total of 150 ng of the pL2R plasmid DNA was incubated at 30°C with 250 nM of Cas3 or one of the nCas3 variants, a crRNA carrying a spacer targeting a 5'-CCC-3' PAM-preceded 32-nt sequence of pL2R, and the Cascade proteins in a reaction buffer containing 2 mM MgCl₂ and 0.5 mM ATP. The reaction products were checked by agarose gel electrophoresis. The crRNA was synthesized from GenScript (Nanjing, China) and listed in electronic supplementary material, table S2.

2.5. Construction and screening of mutants, and curing of genome editing plasmids

The editing plasmids were individually introduced into *Z. mobilis* cells through electroporation. Electroporated cells were spread on RMG agar plates containing spectinomycin at a final concentration of 200 µg ml⁻¹ (RMGSp) and incubated at 30°C until colonies were observed. Mutant candidates were screened by colony PCR using primers listed in electronic supplementary material, table S2. The resulting PCR products were analysed by agarose gel electrophoresis and confirmed by Sanger sequencing (GenScript, Nanjing, China). The genome editing plasmids were cured following the method we previously developed [21].

3. Results

3.1. Inactivation of the helicase domain converts the Cas3 nuclease-helicase into a nickase

Cas3 possesses activities of ssDNA-specific nuclease and ATP-dependent helicase, being responsible for target cleavage and degradation in Type I CRISPR-Cas systems [32]. The nuclease domain of Cas3 initially nicks the target sequence within the ssDNA region of an R-loop generated upon Cascade-binding and crRNA invasion. Subsequently, by consuming ATP, Cas3 unwinds the dsDNA starting at the nicked site via its helicase domain to further provide ssDNA substrate for its nuclease domain, eventually leading to complete target degradation [33,34]. We reasoned that mutating the catalytic residues of the helicase domain might convert Cas3 into a nickase (nCas3), which could no longer unwind the dsDNA due to the loss of its ATPase activity. To verify this assumption, we opted to create nCas3 variants and assess their capability on plasmid DNA nicking.

Amino acid sequence alignment of the Cas3 from *Z. mobilis* (*ZmoCas3*), actually a Cas2–Cas3 fusion encoding by the

cas2/3 gene [21], with several reported Cas3 homologues, had revealed its characteristic helicase motifs (I, II and VI) coordinating ATP binding and hydrolysis [33,35] (figure 1a; electronic supplementary material, figure S1). We therefore designed alanine substitution of conserved residues including K458 located in motif I, D608 in motif II and R887 in motif VI (figure 1b). The variants, as well as the wild-type *ZmoCas3*, could be recombinantly produced in *E. coli* as soluble proteins (figure 1c), and each of which, together with the Cascade–crRNA complex, was incubated with a 3283-bp negatively supercoiled (NS) plasmid, pL2R [21] (electronic supplementary material, table S1), bearing a functional 5'-CCC-3' PAM-preceded protospacer sequence. The treated DNAs were subsequently subjected to electrophoreses using agarose gels. As shown in figure 1d, following nicking the NS plasmid into an open circle (OC) DNA, the wild-type *ZmoCas3* (wt) eventually degraded the plasmid DNA completely; whereas the nCas3 variants gradually nicked the NS plasmid DNA into the OC version. Linear (L) DNAs were also observed, indicative of the occurrence of DSBs. Possibly, in the finite *in vitro* reactions, the nuclease domain of free nCas3 variants could have occasionally touched and cut the opposite strand of the nicked site. These results suggested that all these variants are nCas3s.

3.2. Overexpression of nCas3 has potent killing effect on *Zymomonas mobilis* cells

Having determined the nickase nature of the nCas3 mutants, we next studied whether they could be employed to make DSBs through double nicking for genome editing in *Z. mobilis*. We chose the *ZMO0038* gene as an editing target because it has been ever taken for evaluating the effect of donor sizes on genome editing efficiency in our previous work. Good performance was obtained with one of the tested plasmids, pKO-*ZMO0038-3* [21]. We thus constructed the editing plasmids based on pKO-*ZMO0038-3*. Since paired crRNAs simultaneously targeting two genomic loci were required for double nicking, a new editing plasmid, pKO-*ZMO0038n*, was constructed to bear an artificial CRISPR array consisting of two spacers derived from different strands and three insulating direct repeats. Two different crRNA guides were to be produced from the plasmid-borne artificial CRISPR and were expected to direct a pair of Cascade-nCas3 units to introduce double nicks on different strands of the target, generating a DSB with an overhang (figure 2a).

Initially, taking the convenience of protein expression via an episomal vector, we cloned each gene encoding the wild-type Cas3 or a nCas3 variant to pKO-*ZMO0038n*, yielding four editing plasmids, pKO-*ZMO0038-WT*, pKO-*ZMO0038-K458A*, pKO-*ZMO0038-D608A* and pKO-*ZMO0038-R887A* (electronic supplementary material, table S1). These editing plasmids, and the cloning vector pEZ15Asp as a reference [28], were then individually electroporated into *Z. mobilis* Δ*cas2/3*, a previously constructed *cas2/3* knockout [21]. Only very few transformants could be yielded from transformations with the editing plasmids, showing transformation rates hundreds of times lower than that with the reference plasmid (figure 2b) thereby reflecting a potent killing effect of the wild-type Cas3 and the nCas3s on the host cells.

We speculated that overexpression of the nCas3 variants was toxic to *Z. mobilis* cells. To verify this speculation, we

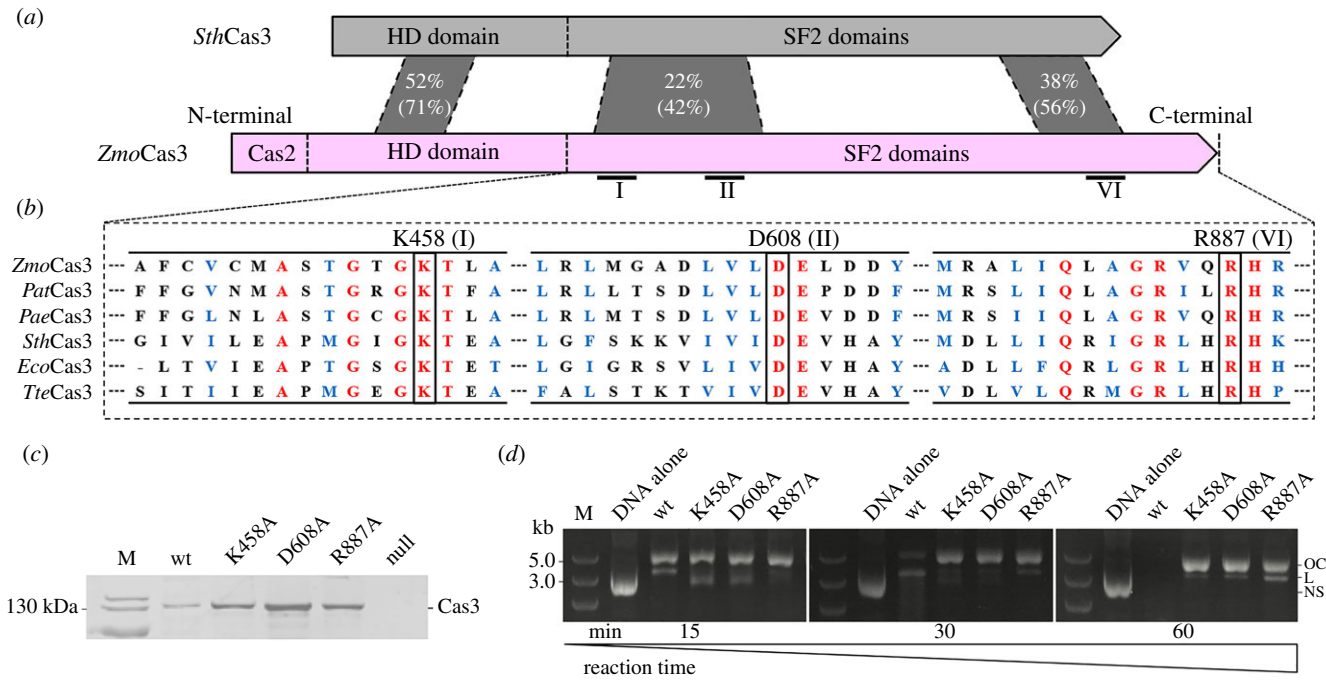


Figure 1. Construction of Cas3 nickase mutants. (a) Schematic organization of Cas3 proteins from *Zymomonas mobilis* ZM4 (*ZmoCas3*) and *Streptococcus thermophilus* DGCC7710 (*SthCas3*). Domain architecture of the Cas3 proteins identified by in silico analysis is shown as pink (*ZmoCas3*) and grey (*SthCas3*) boxes, respectively. Percentage of identical and similar (in parenthesis) residues between conserved sequence blocks is shown. For *ZmoCas3*, Cas2 denotes the N-terminally fused Cas2 domain; HD domain denotes HD-type phosphohydrolase/nuclease domain; SF2 domains denote helicase domains. (b) Locations of the conserved helicase motifs are indicated (I, II and VI) which were identified by alignment of Cas3 proteins from different CRISPR-Cas systems of Type I-E and I-F. Conserved residues characteristic of each motif (K458 of motif I, D608 of motif II and R887 of motif VI, respectively) being subjected to alanine mutagenesis are indicated above the corresponding positions. *Pat*, *Pectobacterium atrosepticum*; *Pae*, *Pseudomonas aeruginosa*; *Eco*, *Escherichia coli* K-12; *Tte*, *Thermobaculum terrenum*. (c) Coomassie blue-stained SDS-PAGE of purified Cas3 proteins expressed in *E. coli*, including the wild-type *ZmoCas3* (wt) and three Cas3 nickase candidates. Null, *E. coli* BL21 (DE3) cells carrying the cloning vector pET28a; M, protein size marker. (d) Analyses of plasmid DNA cleavage by the purified Cas3 proteins as indicated in (c) via electrophoreses using agarose gels. OC, open circle; L, linear; NS, negatively supercoiled; M, DNA size marker.

removed the artificial CRISPR from the editing plasmids, generating three expression plasmids, pEZ-K458A, pEZ-D608A and pEZ-R887A (electronic supplementary material, table S1), with each expressing a corresponding nCas3 whereas no crRNA production. We failed in yielding any transformant from the transformations with these expression plasmids (table 1), suggestive of strong cytotoxicity of the nCas3 nickases *per se* to the *Z. mobilis* cells.

Indeed, it was reported that, if not properly controlled, endonucleases in CRISPR-Cas systems would defend invading genetic elements with the risk of toxic activity against the host [36]. Bacteria have therefore evolved different mechanisms to modulate the activity of Cas nucleases. For example, in Type I-F systems four Cas1 molecules form a complex with two molecules of Cas2–Cas3 fusion to neutralize the nuclease activity of the latter [37]. Reasonably, such a balance might be broken by the overproduction of a Cas3 nickase that disrupted the certain ratio between the subunits.

3.3. A CRISPR-nCas3 genome editing tool is established upon an *in situ* nCas3 variant

In order to attain genome editing with the CRISPR-nCas3 system, we next sought to generate an *in situ* nCas3 by introducing alanine substitution of the D608 residue. To this end, a genome editing plasmid, pNS-*cas2/3* for nucleotide substitutions of *cas2/3*, was designed. By carefully inspecting the coding sequences in the vicinity of the D608 residue, a 5'-

TCC-3' PAM located on the template strand was found, and therefore the 32 nt sequence immediately downstream of it was considered as a protospacer (figure 2c).

Three nucleotide changes were introduced into the donor DNA, that is, C-1T, C3T and T25G, where for clarity, we defined the numbering scheme for protospacer positions as following: the position immediately downstream of PAM is called 1, with subsequent positions being 2, 3, etc., up to 32; while positions within the PAM are referred to as -1, -2 and -3, with -1 being the closest to the protospacer. The C-1T and C3T substitutions interrupted the functional 5'-TCC-3' PAM and the seed sequence to allow for cell surviving after editing, which did not result in any change of protein sequences; while the T25G mutation resulted in altering the original GAT codon for aspartic acid (D) to the GCT codon for alanine (A). In addition, the C3T mutation led to the formation of a TTTAAA restriction site for the *DraI* endonuclease (figure 2c). This allowed us to rapidly screen strains with expected edits by colony PCR amplification of DNA fragments encompassing the edited region followed by *DraI* treatment of the PCR products.

More than 200 transformants were yielded after transforming the pNS-*cas2/3* plasmid into the DRM1 cells [21]. Using the primer set of *cas2/3*-chk-F and *cas2/3*-chk-R (electronic supplementary material, table S2), DNA fragments of 4099 bp were amplified from four randomly picked transformants. The PCR products were then digested with *DraI* followed by electrophoretic analysis using an agarose gel. *DraI* treatment of the reference sample would produce three bands with the sizes of 911 bp, 2121 bp and 1067 bp,

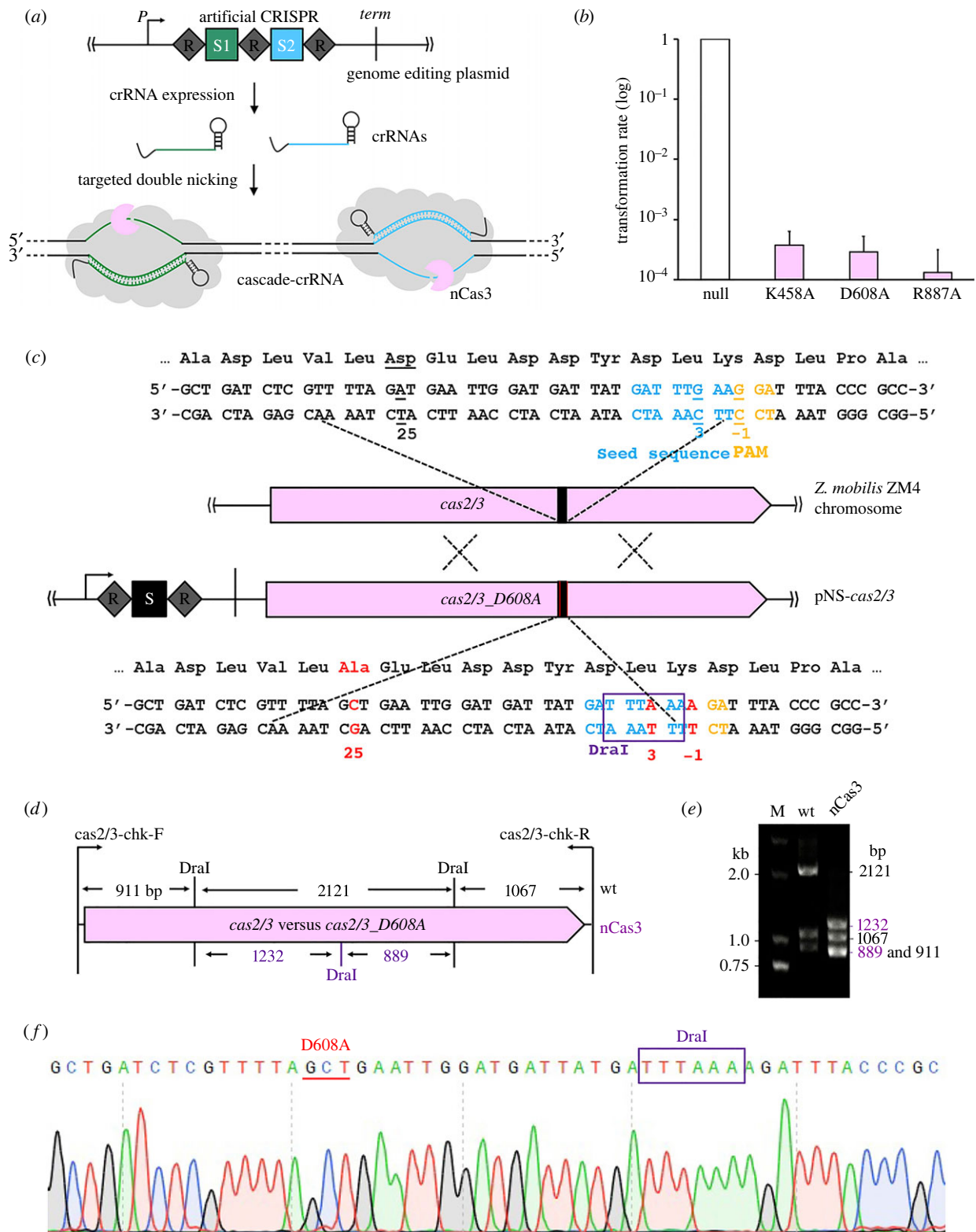


Figure 2. Establishment of a Cascade-nCas3-mediated genome editing tool. (a) A genome editing plasmid contained an artificial CRISPR locus consisting of two spacers (S1 and S2) and three insulating direct repeats (R). Paired self-targeting crRNAs were to be produced from the artificial CRISPR and simultaneously guide Cascade complexes to bind to two target sequences matching S1 and S2, respectively, located on opposing strands. The nCas3 nickases were then recruited to nick the dsDNA within the target sequences. (b) Transforming competent cells of the $\Delta cas2/3$ strain with *ZM00038* knockout plasmids each expressing a Cas3 nickase mutant (K458A, D608A or R887A). Transformation rates are present as relative values to that with a reference plasmid with no Cas3-encoding gene (Null), the latter of which was set to be 1.0. Experiments were performed in triplicate. Error bars represent the standard deviation of the mean. (c) Schematic showing nucleotide substitution of *cas2/3*. The spacer in the genome editing plasmid (pNS-*cas2/3*) for nucleotide substitution of *cas2/3* and the corresponding protospacer in *cas2/3* are indicated as a black box. The PAM motifs are shown in orange while the seed sequence in crane. The designed mutations are indicated as red fonts in *cas2/3_D608A*, whereas the corresponding original nucleotides are underlined in *cas2/3*. The restriction site for *DraI* (TTTAAA) that is to be introduced is framed in a purple box. (d) Schematic showing the digestion sites by *DraI*, among which the newly introduced one is in purple, in the PCR fragments amplified by a primer set of *cas2/3*-chk-F and *cas2/3*-chk-R. The predicted sizes of digestion products are indicated. (e) Electrophoretic analysis of *DraI*-treated colony PCR products amplified from the wild-type strain (wt) and the mutant candidate (nCas3) using primers shown in (d). M, DNA size marker. (f) Representative chromatographs of Sanger sequencing confirming the designed nucleotide substitutions in *cas2/3*.

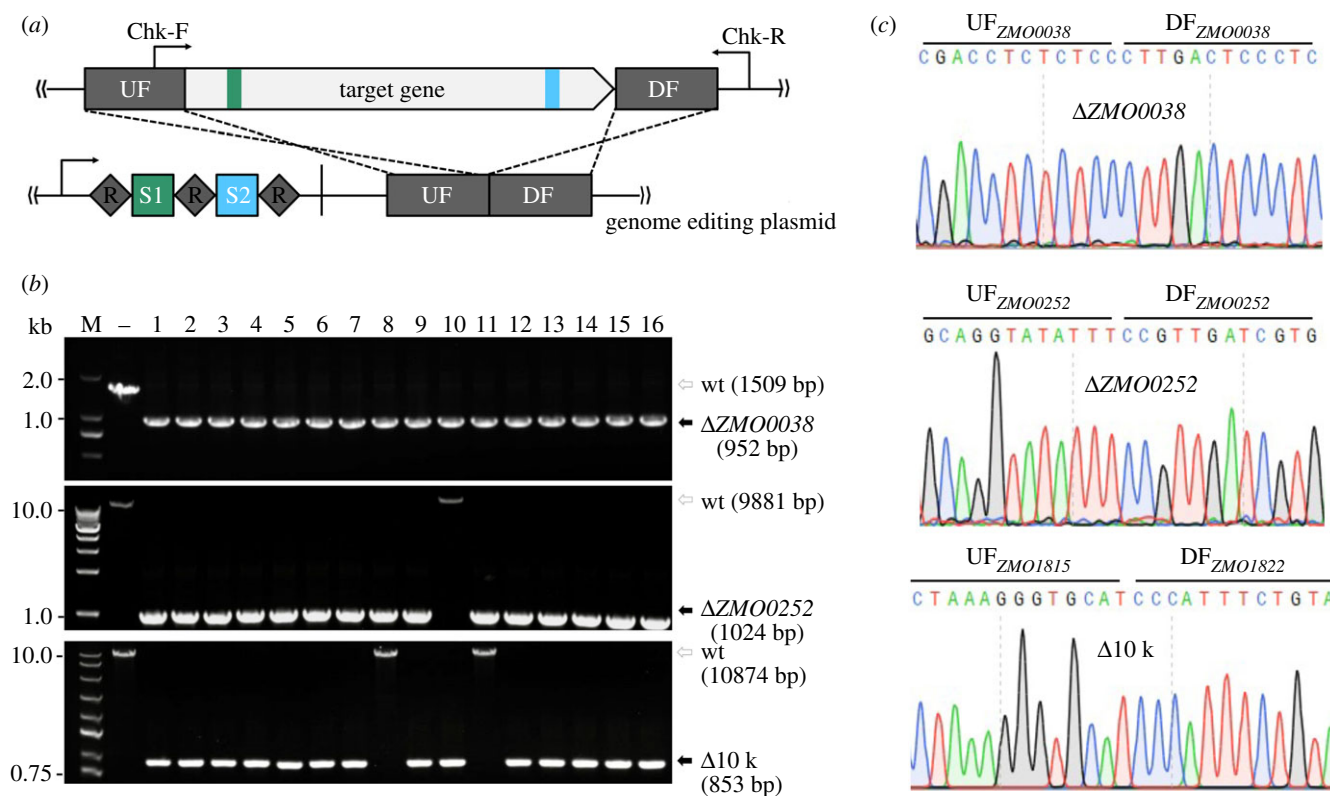


Figure 3. Efficient genome editing using CRISPR-nCas3. (a) Schematic showing design of the genome editing plasmid. An artificial CRISPR expressing two targeting crRNAs and a donor DNA consisting of an up-flanking (UF) and a down-flanking (DF) DNA stretches of the target gene are contained in the all-in-one editing plasmid. (b) Colony PCR screening of deletion mutants of *ZMO0038* (upper panel), *ZMO0252* (middle), an approximately 10 kb genomic fragment (lower panel), respectively, using a gene-specific primer set, Chk-F/ChkR, as indicated in (a). Predicted sizes of PCR products in wild-type (wt) and the expected deletion mutants ($\Delta ZMO0038$, $\Delta ZMO0252$ or $\Delta 10$ k) are indicated with unfilled and filled black arrows, respectively. –, PCR amplification using genomic DNA of *Z. mobilis* ZM4 as a DNA template; M, DNA size marker. (c) Representative chromatographs of Sanger sequencing results.

Table 1. Transformation rates (TR) and editing efficiencies (EE) of various genome editing plasmids in *Z. mobilis* DRM1 and DRM2, respectively. A dash indicates that no value is determined.

plasmid	TR (cfu/ μ g DNA)		EE (% (editing/tested))	
	DRM1	DRM2	DRM1	DRM2
pEZ15A _{sp}	$(3.21 \pm 1.53) \times 10^6$	$(2.33 \pm 1.23) \times 10^6$	—	—
pKO- <i>ZMO0038</i> n	—	$(4.09 \pm 1.14) \times 10^5$	—	100 (16/16)
pKO- <i>ZMO0252</i>	$(9.49 \pm 0.51) \times 10^2$	$(2.47 \pm 0.65) \times 10^5$	37.5 (6/16)	93.75 (15/16)
pDel-10 k	$(1.51 \pm 0.51) \times 10^3$	$(3.02 \pm 0.83) \times 10^4$	31.25 (5/16)	87.5 (14/16)
pRMV	—	$(7.26 \pm 0.25) \times 10^4$	—	93.75 (15/16)

respectively. If the modifications correctly occurred, an additional *Dra*I restriction site would be introduced in the 2121 bp fragment, such that the 2121 bp DNA would be further cut into two fragments of 1232 bp and 889 bp by *Dra*I (figure 2d). The results suggested that the designed *in situ* nCas3 was successfully generated and confirmed via analyses of *Dra*I treatment and Sanger sequencing of the PCR products (figure 2e,f).

The resulting Cas3(D608A) strain, designated *Z. mobilis* DRM2, was then used as the genetic host for CRISPR-nCas3 genome editing. Knockout of *ZMO0038* was attempted in *Z. mobilis* DRM2 cells to assess the capability of CRISPR-nCas3 in genome editing. Transformation of DRM2 competent cells with the pKO-*ZMO0038*n yielded hundreds of transformants,

showing a transformation rate of only about 10-fold lower than that with the reference plasmid (table 1). As expected, after HDR of the DSB generated through double nicking by a pair of Cascade-nCas3 units, deletion of the target gene would occur (figure 3a). Of the obtained transformants, 16 were randomly picked up and analysed by colony PCR and Sanger sequencing genotypic characterization. The results showed that all the tested transformants were identified to harbour the designed deletion of *ZMO0038* (figure 3b,c), giving an editing efficiency of 100% (table 1). Strikingly, 100% editing efficiencies were also yielded in other editing options including nucleotide substitution (electronic supplementary material, figure S2) and *in situ* gene insertion (electronic supplementary material, figure S3).

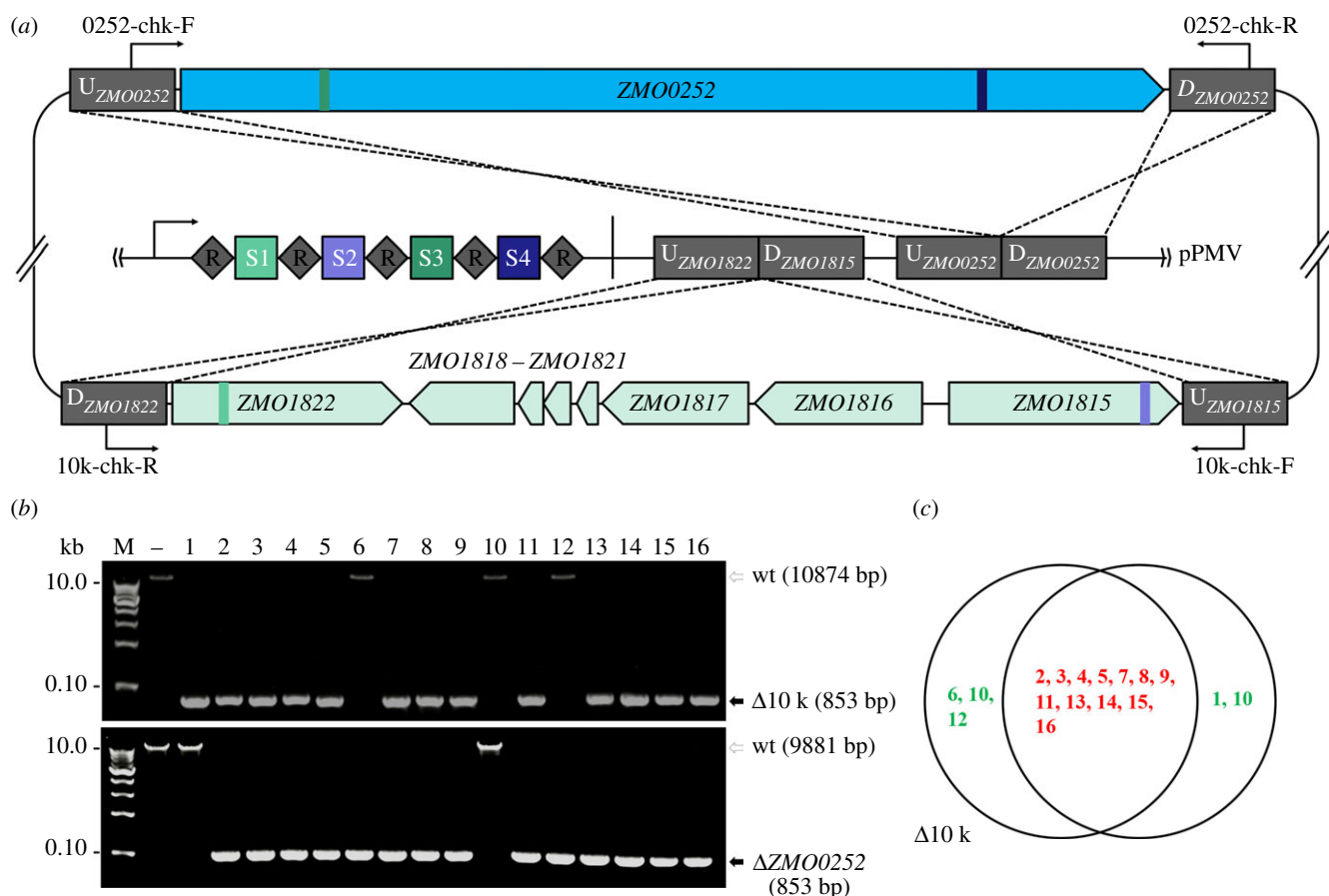


Figure 4. Simultaneous removal of two large genomic fragments using CRISPR-nCas3. (a) Schematic showing design of an 8995-bp *ZMO0052* gene and a approximately 10-kb genomic fragment (spanning genes of *ZMO1815*–*ZMO1822*) deletion. The pRMV plasmid encodes four spacers with S1 and S2 matching sequences within the *ZMO0052* gene while S3 and S4 within the 10-kb region, respectively. DNAs up-flanking (UF) and down-flanking (DF) of the targets were concatenated on the same plasmid as recombination donors. (b) Colony PCR screening of deletion mutants of the 10-kb genomic fragment (upper panel) and *ZMO0052* (lower panel), respectively, using specific primer sets as indicated in (a). Predicted sizes of PCR products in wild-type (wt) and the expected deletion mutants ($\Delta 10$ k or $\Delta ZMO0052$) are indicated with unfilled and filled black arrows, respectively. –, PCR amplification using genomic DNA of *Z. mobilis* ZM4 as a DNA template; M, DNA size marker. (c) Distribution of genomic deletions in the tested transformants. Transformants with both deletions or single deletion are shown in red and green fonts, respectively.

We noted that transformation of DRM2 with pKO-*ZMO0038n* got a rate of about 10-fold higher than that obtained from transformation of DRM1 cells with the pKO-*ZMO0038* plasmid in our previous study [21]. Although in both cases the efficiencies of *ZMO0038* knockout were 100%, the latter was attained by improving pKO-*ZMO0038* transformation rate through destroying a restriction–modification (R–M) system [21]. The further enhanced pKO-*ZMO0038n* transformation rate might reflect a greater capability of the CRISPR-nCas3 in genome editing. To corroborate this, we constructed the pKO-*ZMO0052* plasmid by taking the same strategy as illustrated in figure 3a to delete the 8955 bp *ZMO0052* gene encoding a component of a predicted Type I secretion system [38], looking at whether the CRISPR-nCas3 could also mediate efficient removal of larger genomic fragments. Transforming pKO-*ZMO0052* into DRM2 cells yielded hundreds of transformants. Among them, 16 were randomly chosen 15 of which were identified to be edited cells with the desired genotypes (figure 3b,c), showing an editing efficiency of 93.75% (15/16) (table 1). More importantly, an efficiency of 87.5% was also yielded in the experiment of deleting the 10 021 bp genomic fragment that we took as an editing target in our previous work [21] (figure 3b and table 1). We also used these editing plasmids to perform the same genome editing options in DRM1 cells using the CRISPR-Cas3 tool,

yielding editing efficiencies of 31.25% and 37.5% for deletion of *ZMO0052* and 10 kb fragment, respectively. Particularly, for the 10 kb fragment deletion experiment, both the transformation rates of editing plasmid and the editing efficiency are comparable to that seen in our previous study (table 1). These results demonstrated the overall reproducibility of the observed high-efficiency editing via CRISPR-nCas3.

3.4. CRISPR-nCas3 enables simultaneous removal of large genomic fragments

To further illustrate the versatility of this CRISPR-nCas3-based technology, we opted to use it for simultaneously removing two large genomic loci using a single editing plasmid, pRMV (figure 4a). After electroporating pRMV into DRM2 cells, hundreds of transformants appeared on the selective plate, getting an average transformation rate of $(7.26 \pm 0.25) \times 10^4$ CFU μg^{-1} plasmid DNA (table 1). Of the obtained transformants, 16 were randomly selected for genotypic characterization by colony PCR analysis using specific primer sets listed in electronic supplementary material, table S2. As shown in figure 4b, 13 colonies (i.e. strains 1–5, 7–9, 11 and 13–16) contain the 10 kb fragment deletion, while 14 colonies (i.e. strains 2–9 and 11–16) are *ZMO0052*

knockouts. Collectively, a total of 15 colonies carry at least one deletion, giving an overall editing efficiency of 93.75%. Notably, 12 strains contain both the deletions, showing an engineering efficiency of 75% (figure 4c).

4. Discussion

This work reports the first establishment, to the best of our knowledge, of an advanced CRISPR-nCas3 genome editing method in *Z. mobilis*, which includes a Cas3 nickase. Differently from the Cas9 nucleases which use two nuclease domains, an NHN and a RucV, to respectively cleave the different strands of a dsDNA target [39], Cas3 proteins in Type I systems use only one ssDNA nuclease domain to gradually nick the two strands [33]. As previously demonstrated, Cas3 is recruited to a target upon formation of an ssDNA-containing R-loop through crRNA-directed Cascade-binding and cuts the displaced ssDNA strand first; while cleavage of the crRNA-paired strand requires its ATP-dependent helicase domain to unwind the dsDNA target [33]. This feature allows us to generate the Cas3 nickase mutants by inactivating the helicase domain of the Cas3 nuclease-helicase. Interestingly, as there are several residues essential for the helicase activity [33,35], it is flexible to create different nickase mutants by inactivating any of the essential residues. By contrast, an nCas9 can only be a mutant of either a D10A in RuvC or a H840A in HNH [7]. As derived from an endogenous system, it is more convenient to simultaneously produce crRNA pairs, which is an important requirement for nCas-mediated genome editing [7], through processing the precursor RNAs of the single artificial CRISPR by the Csy4/Cas6f protein [40].

Given the fact that enhanced DNA targeting specificity was achieved with a CRISPR-nCas9 [7], the same should also be true for this CRISPR-nCas3, being of increased genome editing specificity and thus of reduced off-target effect. However, evaluation the off-target effect would be hardly achievable in many prokaryotes. Since eukaryotes possess the NHEJ pathway, they can efficiently repair CRISPR self-targeting introduced DSBs in an error-prone manner, leaving indels in the targeted (both on- and off-target) sites. These ‘scars’ can be found out upon whole-genome sequencing. Most bacteria do not encode the NHEJ system, instead they employ the HDR mechanism to fix DSBs in a precise fashion where donor DNAs are generally required to facilitate homologous recombination. In such bacteria, without supplying donor DNAs, CRISPR-directed chromosomal self-targeting usually leads to cell death. Off-targeting, of course without a homologous template, would be lethal to the bacterial cells as well. It was reported that very few survivors could be identified as escapers carrying mutations that impede the CRISPR-Cas function, such as deletion of the targeting spacer from the CRISPR array through recombination between identical repeats [41,42]. Very recently, Xu *et al.* demonstrated that all the bacterial cells escaped from self-targeting by a Type I-F system carried mutations in the key components of the Cascade, and more importantly, they found that genome-targeting by the Type I-F system is more specific than that by a Type II Cas9 [43]. Also, as the nCas9 showed an obvious advantage in helping base editing over other Cas9 variants [8], we envision that nCas3-based toolkits, such as base editors, would be soon available for various

bacteria harbouring an active Type I CRISPR-Cas. Type I-F systems have relatively fewer Cas components among the Type I subtypes [4], and they are thereby readily potable for heterologous genome editing in other organisms [43].

Significantly elevated editing efficiencies (near 100%) were observed in the application of CRISPR-nCas3 tool for genome editing including simultaneous deletion of large genomic fragments. Our previous demonstrations showed that only up to 50% efficiency for removal of one large genome fragment could be attained, and simultaneous deleting multiple small DNA stretches yielded an efficiency of 18.75%. We noted that for simultaneous removal two large genome fragments, the transformation rate of the editing plasmid and the engineering efficiency are at the same level as that observed for deletion of either of them, indicating that simultaneously deleting more genomic targets would be also efficiently achieved with this CRISPR-nCas3 tool. Previously, the processive DNA degradation activity of Cas3 nucleases has been harnessed for long-range genomic deletions in bacteria [16] and human embryonic stem cells [23], albeit in an uncontrollable manner. Here the nCas3 nickase, combined with the host HDR system, has enabled precise deletion of large-scale genomic fragments. Particularly, this feature might be of great help for minimal genome construction in bacteria carrying compact genomes.

Since editing efficiencies rely largely on the repair rates of DSBs by the host’s repair systems, together with the fact that *Z. mobilis* lacks an NHEJ system, the enhancement of editing efficiency might be due to faster repair of the DSBs by the HDR systems, thereby letting more cells be recovered from self-targeting. It is possible that each of the DSB ends produced by nCas3-mediated double nicking carries an overhang structure, which might be more efficiently sensed and bound by RecA to initial DSB repair [44]. Another possibility could be that the overhangs might trigger or activate an alternative repair system with an even higher efficacy, as bacteria generally possess multiple HDR systems [45] (e.g. *Z. mobilis* ZM4 encodes at least two HDR mechanisms, i.e. an AddAB and a RecF [46]). By the way, this work offers an easy method to produce DSBs at defined genomic locations with expected terminal structures for studying HDR mechanisms in bacteria *in vivo*. Other possibilities include that double nicking by nCas3 might be lesser toxic than processive degradation by Cas3 nuclease-helicase, thus enabling more cells to be recovered. Bacteria are generally sensitive to CRISPR-mediated chromosomal self-targeting. Potent CRISPR self-targeting may lead to failure in yielding any recovered cells with the designed edits. Indeed, in this work, transformation of the same editing plasmid into cells with an nCas3 background yielded about 20-fold higher rate than into those with a Cas3 background (table 1). In the future, comprehensive studies combining structural, genetic and biochemical analyses on the HDR mechanisms in *Z. mobilis* may offer molecular explanations for the observed phenomenon, as well as mechanistic insights for directing high-efficiency genome editing.

Conclusively, we have created a Type I-F CRISPR-nCas3-based technology that represents currently the most efficient and straightforward genome engineering tool for the important industrial bacterium *Z. mobilis*. It has allowed us to achieve highly efficient removal of genomic fragments in a large-scale manner in *Z. mobilis*, and hence would expedite the development and improvement of this bacterium as an ideal chassis for synthetic biology researches. This study

expands the available tools for CRISPR-mediated genome engineering and may serve as a framework for future development of next-generation CRISPR-Cas technologies.

Data accessibility. The authors declare that the main data supporting the findings of this work are available within the article and additional data are provided in electronic supplementary material [47].

Authors' contributions. W.P., Y.Z. and S.Y. designed the research; Y.H., Q.W. and J.L. performed the experiments; W.P., Y.H. and Y.Z. wrote the manuscript. All authors contributed to data analyses, and read, revised and approved the final manuscript. All authors

gave final approval for publication and agreed to be held accountable for the work performed therein.

Competing interests. We declare we have no competing interests.

Funding. This work was supported by the Scientific Research Program of Hubei Provincial Department of Education (grant no. Q20161007), the National Key Technology Research, the Development Program of China (grant no. 2018YFA0900300), the National Natural Science Foundation of China (grant no. U1932141), the Hubei Technical Innovation Special Fund (grant nos. 2019AHB055 and 2018ACA149) and the Innovation Base for Introducing Talents of Discipline of Hubei Province (grant no. 2019BJH021). W.P. acknowledges the support from the State Key Laboratory of Biocatalysis and Enzyme Engineering.

References

- Barrangou R, Fremaux C, Deveau H, Richards M, Boyaval P, Moineau S, Romero DA, Horvath P. 2007 CRISPR provides acquired resistance against viruses in prokaryotes. *Science* **315**, 1709–1712. (doi:10.1126/science.1138140)
- Brouns SJ *et al.* 2008 Small CRISPR RNA guide antiviral defense in prokaryotes. *Science* **321**, 960–964. (doi:10.1126/science.1159689)
- Anzalone AV, Koblan LW, Liu DR. 2020 Genome editing with CRISPR-Cas nucleases, base editors, transposases and prime editors. *Nat. Biotechnol.* **38**, 824–844. (doi:10.1038/s41587-020-0561-9)
- Makarova KS *et al.* 2020 Evolutionary classification of CRISPR-Cas systems: a burst of Class 2 and derived variants. *Nat. Rev. Microbiol.* **18**, 67–83. (doi:10.1038/s41579-019-0299-x)
- Barrangou R, Doudna JA. 2016 Applications of crispr technologies in research and beyond. *Nat. Biotechnol.* **34**, 933–941. (doi:10.1038/nbt.3659)
- Graham DB, Root DE. 2015 Resources for the design of CRISPR gene editing experiments. *Genome Biol.* **16**, 260. (doi:10.1186/s13059-015-0823-x)
- Ran FA *et al.* 2013 Double nicking by RNA-guided CRISPR Cas9 for enhanced genome editing specificity. *Cell* **154**, 1380–1389. (doi:10.1016/j.cell.2013.08.021)
- Nishida K *et al.* 2016 Targeted nucleotide editing using hybrid prokaryotic and vertebrate adaptive immune systems. *Science* **353**, aaf8729. (doi:10.1126/science.aaf8729)
- Vento JM, Crook N, Beisel CL. 2019 Barriers to genome editing with CRISPR in bacteria. *J. Ind. Microbiol. Biotechnol.* **46**, 1327–1341. (doi:10.1007/s10295-019-02195-1)
- Xu Z, Li Y, Li M, Xiang H, Yan A. 2021 Harnessing the type I CRISPR-Cas systems for genome editing in prokaryotes. *Environ. Microbiol.* **23**, 542–558. (doi:10.1111/1462-2920.15116)
- Zheng Y *et al.* 2020 Endogenous Type I CRISPR-Cas: from foreign DNA defense to prokaryotic engineering. *Front. Bioeng. Biotechnol.* **8**, 62. (doi:10.3389/fbioe.2020.00062)
- Li Y, Pan S, Zhang Y, Ren M, Feng M, Peng N, Chen L, Liang YX, She Q. 2016 Harnessing type I and type III CRISPR-Cas systems for genome editing. *Nucleic Acids Res.* **44**, e34. (doi:10.1093/nar/gkv1044)
- Cheng F, Gong L, Zhao D, Yang H, Zhou J, Li M, Xiang H. 2017 Harnessing the native type I-B CRISPR-Cas for genome editing in a polyploid archaeon. *J. Genet. Genom.* **44**, 541–548. (doi:10.1016/j.jgg.2017.09.010)
- Pyne ME, Bruder MR, Moo-Young M, Chung DA, Chou CP. 2016 Harnessing heterologous and endogenous CRISPR-Cas machineries for efficient markerless genome editing in *Clostridium*. *Sci. Rep.* **6**, 25666. (doi:10.1038/srep25666)
- Zhang J, Zong W, Hong W, Zhang Z-T, Wang Y. 2018 Exploiting endogenous CRISPR-Cas system for multiplex genome editing in *Clostridium tyrobutyricum* and engineer the strain for high-level butanol production. *Metab. Eng.* **47**, 49–59. (doi:10.1016/j.ymben.2018.03.007)
- Csorgo B, Leon LM, Chau-Ly IJ, Vasquez-Rifo A, Berry JD, Mahendra C, Crawford ED, Lewis JD, Bondy-Denomy J. 2020 A compact cascade-Cas3 system for targeted genome engineering. *Nat. Methods* **17**, 1183–1190. (doi:10.1038/s41592-020-00980-w)
- Canez C, Selle K, Goh YJ, Barrangou R. 2019 Outcomes and characterization of chromosomal self-targeting by native CRISPR-Cas systems in *Streptococcus thermophilus*. *FEMS Microbiol. Lett.* **366**, fnz105. (doi:10.1093/femsle/fnz105)
- Hidalgo-Cantabrana C, Goh YJ, Pan M, Sanozky-Dawes R, Barrangou R. 2019 Genome editing using the endogenous type I CRISPR-Cas system in *Lactobacillus crispatus*. *Proc. Natl Acad. Sci. USA* **116**, 15 774–15 783. (doi:10.1073/pnas.1905421116)
- Vercoe RB *et al.* 2013 Cytotoxic chromosomal targeting by CRISPR/Cas systems can reshape bacterial genomes and expel or remodel pathogenicity islands. *PLOS Genet.* **9**, e1003454. (doi:10.1371/journal.pgen.1003454)
- Xu Z *et al.* 2019 Native CRISPR-Cas-mediated genome editing enables dissecting and sensitizing clinical multidrug-resistant *P. aeruginosa*. *Cell Rep.* **29**, 1707–1717.e1703. (doi:10.1016/j.celrep.2019.10.006)
- Zheng Y *et al.* 2019 Characterization and repurposing of the endogenous Type I-F CRISPR-Cas system of *Zymomonas mobilis* for genome engineering. *Nucleic Acids Res.* **47**, 11 461–11 475. (doi:10.1093/nar/gkv940)
- Osakabe K *et al.* 2020 Genome editing in plants using CRISPR type I-D nuclease. *Commun. Biol.* **3**, 648. (doi:10.1038/s42003-020-01366-6)
- Dolan AE, Hou Z, Xiao Y, Gramelspacher MJ, Heo J, Howden SE, Freddolino PL, Ke A, Zhang Y. 2019 Introducing a spectrum of long-range genomic deletions in human embryonic stem cells using type I CRISPR-Cas. *Mol. Cell* **74**, 936–950; e935. (doi:10.1016/j.molcel.2019.03.014)
- Morisaka H *et al.* 2019 CRISPR-Cas3 induces broad and unidirectional genome editing in human cells. *Nat. Commun.* **10**, 5302. (doi:10.1038/s41467-019-13226-x)
- Cameron P *et al.* 2019 Harnessing type I CRISPR-Cas systems for genome engineering in human cells. *Nat. Biotechnol.* **37**, 1471–1477. (doi:10.1038/s41587-019-0310-0)
- Pickar-Oliver A *et al.* 2019 Targeted transcriptional modulation with type I CRISPR-Cas systems in human cells. *Nat. Biotechnol.* **37**, 1493–1501. (doi:10.1038/s41587-019-0235-7)
- Chen Y *et al.* 2020 Repurposing type I-F CRISPR-Cas system as a transcriptional activation tool in human cells. *Nat. Commun.* **11**, 3136. (doi:10.1038/s41467-020-16880-8)
- Yang S, Mohagheghi A, Franden MA, Chou Y-C, Chen X, Dowe N, Himmel ME, Zhang M. 2016 Metabolic engineering of *Zymomonas mobilis* for 2,3-butanediol production from lignocellulosic biomass sugars. *Biotechnol. Biofuels* **9**, 189. (doi:10.1186/s13068-016-0606-y)
- Okamoto T, Nakamura K. 1992 Simple and highly efficient transformation method for *Zymomonas mobilis* - electroporation. *Biosci. Biotechnol. Biochem.* **56**, 833. (doi:10.1271/bbb.56.833)
- Horton RM, Cai ZL, Ho SN, Pease LR. 2013 Gene splicing by overlap extension: tailor-made genes using the polymerase chain reaction. *BioTechniques* **8**, 528–535 (November 1990). *BioTechniques* **54**, 129–133. (doi:10.2144/000114017)
- Xia Y, Li K, Li J, Wang T, Gu L, Xun L. 2019 T5 exonuclease-dependent assembly offers a low-cost method for efficient cloning and site-directed mutagenesis. *Nucleic Acids Res.* **47**, e15. (doi:10.1093/nar/gky1169)
- He L, St John James M, Radovic M, Ivancic-Bace I, Bolt EL. 2020 Cas3 protein—a review of a

- multi-tasking machine. *Genes (Basel)* **11**, 208. (doi:10.3390/genes11020208)
33. Sinkunas T, Gasiunas G, Fremaux C, Barrangou R, Horvath P, Siksnys V. 2011 Cas3 is a single-stranded DNA nuclease and atp-dependent helicase in the CRISPR/Cas immune system. *EMBO J.* **30**, 1335–1342. (doi:10.1038/emboj.2011.41)
 34. Hidalgo-Cantabrana C, Barrangou R. 2020 Characterization and applications of type I CRISPR-Cas systems. *Biochem. Soc. Trans.* **48**, 15–23. (doi:10.1042/BST20190119)
 35. Gong B, Shin M, Sun J, Jung C-H, Bolt EL, Van Der Oost J, Kim J-S. 2014 Molecular insights into DNA interference by CRISPR-associated nuclease-helicase Cas3. *Proc. Natl Acad. Sci. USA* **111**, 16 359–16 364. (doi:10.1073/pnas.1410806111)
 36. Leon LM, Mendoza SD, Bondy-Denomy J. 2018 How bacteria control the CRISPR-Cas arsenal. *Curr. Opin. Microbiol.* **42**, 87–95. (doi:10.1016/j.mib.2017.11.005)
 37. Rollins MF, Chowdhury S, Carter J, Golden SM, Wilkinson RA, Bondy-Denomy J, Lander GC, Wiedenheft B. 2017 Cas1 and the Csy complex are opposing regulators of Cas2/3 nuclease activity. *Proc. Natl Acad. Sci. USA* **114**, E5113–E5121. (doi:10.1073/pnas.1620722114)
 38. Zhang YP *et al.* 2019 Multiomic fermentation using chemically defined synthetic hydrolyzates revealed multiple effects of lignocellulose-derived inhibitors on cell physiology and xylose utilization in *Zymomonas mobilis*. *Front. Microbiol.* **10**, 2596. (doi:10.3389/fmicb.2019.02596)
 39. Cong L *et al.* 2013 Multiplex genome engineering using CRISPR/Cas systems. *Science* **339**, 819–823. (doi:10.1126/science.1231143)
 40. Przybilski R, Richter C, Gristwood T, Clulow JS, Vercoe RB, Fineran PC. 2011 Csy4 is responsible for CRISPR RNA processing in *Pectobacterium atrosepticum*. *RNA Biol.* **8**, 517–528. (doi:10.4161/rna.8.3.15190)
 41. Gudbergsdottir S, Deng L, Chen Z, Jensen JVK, Jensen LR, She Q, Garrett RA. 2011 Dynamic properties of the *Sulfolobus* CRISPR/Cas and *crispr/cmr* systems when challenged with vector-borne viral and plasmid genes and protospacers. *Mol. Microbiol.* **79**, 35–49. (doi:10.1111/j.1365-2958.2010.07452.x)
 42. Stout EA, Sanozky-Dawes R, Goh YJ, Crawley AB, Klaenhammer TR, Barrangou R. 2018 Deletion-based escape of CRISPR-Cas9 targeting in *Lactobacillus gasseri*. *Microbiology (Reading)* **164**, 1098–1111. (doi:10.1099/mic.0.000689)
 43. Xu Z, Li Y, Cao H, Si M, Zhang G, Woo PCY, Yan A. 2021 A transferrable and integrative Type I-F cascade for heterologous genome editing and transcription modulation. *Nucleic Acids Res.* **49**, e94. (doi:10.1093/nar/gkab521)
 44. Wigley DB. 2013 Bacterial DNA repair: recent insights into the mechanism of recbcd, addab and adnab. *Nat. Rev. Microbiol.* **11**, 9–13. (doi:10.1038/nrmicro2917)
 45. Bernheim A, Bikard D, Touchon M, Rocha EPC. 2019 A matter of background: DNA repair pathways as a possible cause for the sparse distribution of CRISPR-Cas systems in bacteria. *Phil. Trans. R. Soc. B* **374**, 20180088. (doi:10.1098/rstb.2018.0088)
 46. Yang S *et al.* 2018 Complete genome sequence and the expression pattern of plasmids of the model ethanologen *Zymomonas mobilis* ZM4 and its xylose-utilizing derivatives 8b and 2032. *Biotechnol. Biofuels* **11**, 125. (doi:10.1186/s13068-018-1116-x)
 47. Hao Y, Wang Q, Li J, Yang S, Zheng Y, Peng W. 2022 Double nicking by RNA-directed Cascade-nCas3 for high-efficiency large-scale genome engineering. Figshare.